

THE PHYSICAL REVIEW

A journal of experimental and theoretical physics established by E. L. Nichols in 1893

SECOND SERIES, VOL. 137, No. 6B

22 MARCH 1965

Lifetimes of 1^- States in Sm^{148} and Sm^{152} †

F. R. METZGER

Bartol Research Foundation of The Franklin Institute, Swarthmore, Pennsylvania

(Received 5 November 1964)

Sources of $(\text{Pm}^{148})_2\text{O}_3$ and $(\text{Eu}^{152})_2\text{O}_3$, moving at the high linear velocities available with ultracentrifuges, provided the resonant gamma radiation for the excitation of the 1.46-MeV 1^- level in Sm^{148} and the 0.96-MeV 1^- level in Sm^{152} . The partial width Γ_0 for the 0.96-MeV $E1$ ground-state transition in Sm^{152} was determined in a self-absorption experiment as $\Gamma_0 = (7.3 \pm 0.6) \times 10^{-3}$ eV. With a branching ratio $\Gamma_{0.96}/\Gamma_{0.84} = 0.77$, this leads to a mean life $\tau_{\text{level}}(0.96 \text{ MeV}) = (3.9 \pm 0.4) \times 10^{-14}$ sec. The scattering data from Sm^{148} were analyzed, using slowing-down information obtained from a study of the shape of the 0.96-MeV Sm^{152} emission line, and a mean life $\tau_{\text{level}}(1.46 \text{ MeV}) = (1.4_{-0.3}^{+0.6}) \times 10^{-13}$ sec was obtained. These results show that the $E1$ transitions from the 1^- states in Sm^{148} and Sm^{152} are considerably retarded, the retardation for the transitions in the spherical nucleus Sm^{148} being almost 1 order of magnitude larger than that for the $E1$ transitions in the deformed nucleus Sm^{152} .

I. INTRODUCTION

SEVERAL even-even rare-earth nuclei are known¹ to have 1^- states with excitation energies of the order of 1 MeV. The character of these states is rather uncertain,¹ and it appeared of interest to obtain additional experimental information concerning them. So far, the lifetimes of two 1^- levels had been investigated. A value of $\tau = (4.7 \pm 0.5) \times 10^{-14}$ sec was reported² for the mean life of the 0.96-MeV excited state in Sm^{152} , while a lower limit³ of $(2.0 \pm 0.4) \times 10^{-14}$ sec and a range⁴ $1.4 \times 10^{-14} < \tau < 3.4 \times 10^{-14}$ sec were established for the 2.18-MeV state in Nd^{144} . In all cases, resonance-fluorescence techniques were used. For the state in Sm^{152} , no special effort was necessary in order to establish the resonance condition because the Doppler effect due to the preceding radiation plus the thermal agitation are sufficient to compensate for the recoil energy losses. For the 2.18-MeV transition in Nd^{144} , on the other hand, the beta recoil is not sufficiently large, and the overlap of emission and absorption line is due to the tail of the Lorentz shape of these lines. If the lifetime is a few times 10^{-14} sec or longer, this contribution is too small to be observed. For the 1.46-MeV transition in Sm^{148} , the situation is slightly more favora-

able than for Nd^{144} because the maximum beta recoil is just about sufficient for compensation. In spite of this, preliminary experiments using Pm^{148} sources were unsuccessful, indicating that the mean life of the 1.46 MeV level in Sm^{148} was of the order of, or larger than, 10^{-13} sec. From Fig. 1, which depicts the Sm^{148} situation in the absence of slowing down, it becomes clear that the resonance effect could be drastically increased if emitter and absorber were moving toward each other, i.e., if the gap separating the emission line from the absorption line were reduced. This aim can be achieved, since presently available ultracentrifuge rotors⁵ provide Doppler shifts of $\Delta E/E = 4 \times 10^{-6}$, which is of the order of magnitude of the gap $\Delta E_R/E = 10.6 \times 10^{-6}$. In Fig. 1 the dashed line represents the shifted relative position of the absorption line for a convenient source speed of 1.07×10^5 cm/sec (2800 rps). For this speed the increase in the overlap of emission and absorption lines, and hence the increase in the resonance effect, amounts to almost two orders of magnitude. In view of this large gain in sensitivity it was decided to carry out such an experiment with Sm^{148} .

The evaluation of the observed resonance scattering in terms of the lifetime of the 1.46-MeV state of Sm^{148} would be straightforward if the situation depicted in Fig. 1 prevailed. Unfortunately, the shape of the emission line shown in Fig. 1 is only realized if the beta recoil is fully effective, i.e., if the slowing down of the

† Work supported by the National Science Foundation.

¹ M. Sakai, Phys. Letters 3, 338 (1963).

² G. G. Shute and B. S. Sood, Proc. Roy. Soc. (London) **A257**, 52 (1960).

³ P. Rice-Evans, Proc. Phys. Soc. (London) **A82**, 914 (1963).

⁴ J. P. Blanc, M. Lambert, and C. F. Perdrisat, Helv. Phys. Acta **36**, 820 (1963).

⁵ See, for instance, F. R. Metzger and H. Langhoff, Phys. Rev. **132**, 1753 (1963).

excited nuclei prior to the emission of the 1.46-MeV gamma radiation is negligible. For a level with a mean life of the order of 10^{-13} sec this is no longer true if solid or liquid sources are used, and the knowledge of the slowing-down behavior enters into the evaluation of the experimental data. For the range of recoil energies of a few electron volts to tens of electron volts, the experimental slowing-down information comes from resonance fluorescence experiments. Of these, only two had investigated the shape of the collision-modified emission line, one for Sm^{152} ,⁶ the other for Re^{187} .⁷ The experiment with Sm^{152} appeared to be in conflict with the expectation based on other slowing down data.^{2,8} Since information concerning Sm^{152} is especially pertinent to the case of Sm^{148} , it was decided to repeat the study of Sm^{152} . Another reason was the disagreement between two values reported for the lifetime of the 0.96-MeV level in Sm^{152} , one determined in a self-absorption study,² the other in a scattering experiment utilizing Compton-scattered Co^{60} gamma rays as the exciting radiation.⁹

In the following sections, we shall describe the experimental procedures, analyze in succession the self-absorption data obtained with Sm^{152} , the scattering from Sm^{152} measured at different rotor speeds, and the scattering from Sm^{148} . The information on $E1$ transition probabilities in Sm^{148} and Sm^{152} obtained in this way will be summarized and discussed in the final section.

II. EXPERIMENTAL PROCEDURES

All the experiments were carried out using titanium alloy rotors in a conventional scattering geometry.⁵ The samarium metal scatterer measured $2\frac{1}{4} \times 1\frac{1}{2} \times \frac{1}{8}$ in. Neodymium metal served as the comparison scatterer. Except for the angular distribution measurement with Sm^{148} , all experiments were carried out with a scattering angle of 105° , this choice combining good shielding with a favorable solid angle.

A source of 5.4-day Pm^{148} , prepared by neutron irradiation of a few tenths of a milligram of $(\text{Pm}^{147})_2\text{O}_3$ powder in the Oak Ridge National Laboratory Research Reactor, provided the exciting 1.46-MeV gamma radiation for the study of Sm^{148} . In the case of Sm^{152} , 9.3-h Eu^{152} , prepared by neutron irradiation of Eu_2O_3 , was used.

The output of the 3-in. \times 3-in. NaI detector system was connected to a 400-channel RIDL analyzer. A lead absorber, $\frac{1}{4}$ in. thick, placed in front of the detector, removed the intense low-energy component from the scattered radiation.

With the Pm^{148} source, pulse-height distributions

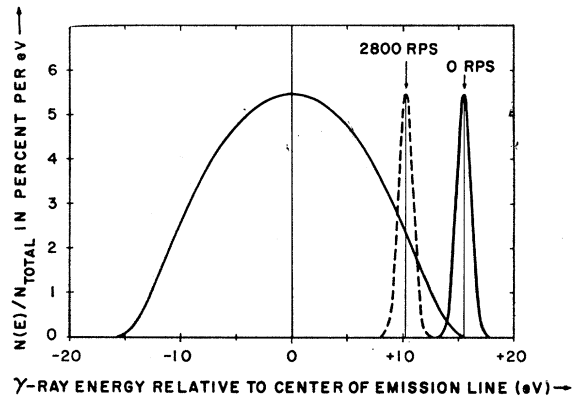


Fig. 1. The broad curve depicts the collision-free shape of the 1.46-MeV gamma line emitted by an ensemble of Pm^{148} nuclei. With source and scatterer at rest, the absorption line ("0 RPS") is located near the high-energy end point of the emission line. For a rotor speed of 2800 revolutions per second, corresponding to a tangential velocity of 1.07×10^5 cm/sec, the absorption line (dashed curve) exhibits considerable overlap with the emission line.

were measured for both scatterers with the source at rest, and for source velocities of 1.07, 0.92, 0.76, 0.61, and 0.46 km/sec. A typical pair of pulse height distributions is shown in Fig. 2. The 1.46-MeV line is well resolved from the background, which also exhibits a 1.46-MeV peak due to insufficient shielding of the crystal against the direct radiation from the rotating source. For the evaluation of the scattering data, the counts in channels 68 through 74 were added.

An additional run was carried out with a scattering angle of 130° . The purpose of this measurement was to ascertain that the resonance scattering originated from a level with spin 1 and not from a level with spin 2.

For the Sm^{152} level, the counting rates were two orders of magnitude larger than for the Sm^{148} level. Consequently, it was possible to obtain significant data at 20 different source speeds with one Eu^{152} source. A

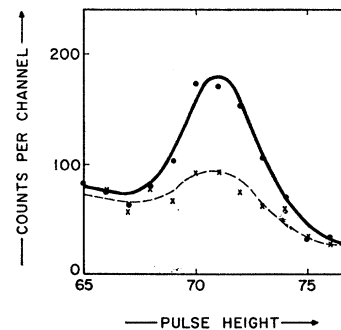


Fig. 2. Resonance scattering from Sm^{148} at a source velocity of 1.07×10^5 cm/sec. The pulse-height distributions of the radiation scattered from Sm (circles) and from Nd (crosses) are compared in the region of the 1.46-MeV full-energy peak. The peak observed with the Nd comparison scatterer was also observed in the absence of any scatterer and is attributed to insufficient shielding of the detector.

⁶ P. B. Moon and B. S. Sood, Proc. Roy. Soc. (London) A257, 44 (1960).

⁷ H. Langhoff, Phys. Rev. 135, B1 (1964).

⁸ S. Ofer and A. Schwarzschild, Phys. Rev. Letters 3, 384 (1959).

⁹ G. K. Tandon and J. A. McIntyre, Bull. Am. Phys. Soc. 9, 152 (1964).

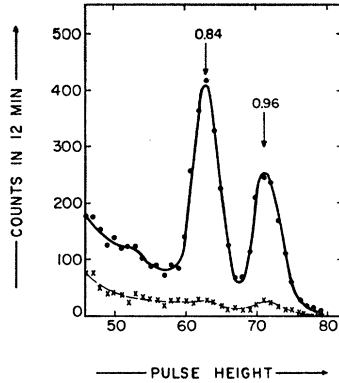


FIG. 3. Resonance scattering from Sm^{152} at a source velocity of 1.10×10^5 cm/sec. The pulse-height distribution of the radiation scattered from Sm (circles) exhibits two peaks, since the 0.96-MeV 1^- level decays to the 0.12-MeV 2^+ state as well as to the ground state of Sm^{152} . The background counting rate (crosses) was measured with a Nd scatterer.

typical pair of pulse height distributions is shown in Fig. 3. In this case, the counts in channels 58 through 78 were added and these sums were used for the determination of the shape of the resonance effect versus source velocity.

For the redetermination of the lifetime of the 0.96-MeV level in Sm^{152} , the scattering data alone were not of much use since they were affected by collisions. A self-absorption experiment was, therefore, carried out at a source speed of 1.02 km/sec, because at this speed the scattering effect was several times larger than the effect for the Eu^{152} source at rest, and the emission line was reasonably smooth. Absorbers of Sm_2O_3 and Nd_2O_3 , with a surface density of 2.34 g/cm², were alternately placed into the path of the incident beam, and the change in the scattering from the Sm scatterer was measured. To insure that the measured absorption was not affected by resonance radiation from the absorber reaching the detector, additional measurements were carried out using the comparison Nd scatterer and interchanging the absorbers.

III. ANALYSIS OF EXPERIMENTAL DATA

A. Self-Absorption in Sm^{152}

If the resonance scattering counting rates with the Sm_2O_3 and Nd_2O_3 absorbers are denoted by C_{Sm} and C_{Nd} , the fractional change $R = (C_{\text{Nd}} - C_{\text{Sm}}) / C_{\text{Nd}}$ is a measure of the self-absorption, provided the absorbers have been matched with respect to their nonresonant absorption. The experimental value for R , obtained in 7 h of centrifuge operation, is $R = 0.119 \pm 0.008$. In first approximation,¹⁰ R is related to the partial width Γ_0 for the ground-state transition by

$$R = n_a t (g_2/g_1) \lambda^2 \Gamma_0 \times \frac{1}{4} [\pi (\Delta_a^2 + \Delta_s^2)]^{-1/2}, \quad (1)$$

¹⁰ F. R. Metzger, Phys. Rev. 103, 983 (1956); and in *Progress in Nuclear Physics*, edited by O. R. Frisch (Pergamon Press, Ltd., London, 1959), Vol. 7, p. 54.

where n_a is the number of resonant nuclei per cm³ of the absorber, t the absorber thickness in cm, g_2/g_1 the ratio of the statistical factors of excited state and ground state, respectively, λ the wavelength of the gamma radiation, and Δ_a and Δ_s are the thermal Doppler widths¹⁰ of absorber and scatterer. Using effective temperatures¹⁰ of 306°K for both, one calculates $\Delta_a = \Delta_s = 0.586$ eV. With $g_2/g_1 = 3$, $n_a t = 2.15 \times 10^{21}$ Sm^{152} nuclei per cm², and $\lambda^2 = 1.66 \times 10^{20}$ cm², the experimental absorption leads to a partial width $\Gamma_0 = 6.53 \times 10^{-3}$ eV. A more accurate evaluation, in addition to considering higher terms, has to take into account the effect of the finite thickness of the scatterer on the measured self absorption. Using the Doppler form¹⁰—as is justified by the small value of Γ_0 —the following expression for R is obtained:

$$R = 1 - \frac{\int_0^D [e^{-n_x(\sigma_e \eta + \sigma_e' \xi)} S(n_s K_s \eta x + n_a K_a t)] dx}{\int_0^D [e^{-n_x(\sigma_e \eta + \sigma_e' \xi)} S(n_s K_s \eta x)] dx}, \quad (2)$$

where

$$S(z) = \sum_{m=0}^{\infty} (-1)^m z^m / [m!(m+1)^{1/2}]$$

and

$$K_s = g \lambda^2 \Gamma_0 / 4\pi^{1/2} \Delta_s.$$

In Eq. (2), n is the total number of nuclei per cm³ of the scatterer, while n_s is the number of resonant nuclei per cm³ of the scatterer. The total electronic cross section for the incident radiation is denoted by σ_e , the poor geometry cross section for the outgoing radiation by σ_e' . σ_e' was obtained by subtracting 20% of the Compton cross section from σ_e . The integration was carried out over the depth x of the scatterer, D being the total depth or thickness. η and ξ take into account the oblique entrance and exit of the gamma rays.

The right-hand side of Eq. (2) was evaluated for Γ_0 values ranging from 6.6×10^{-3} to 8.2×10^{-3} eV; in Fig. 4, the calculated self absorptions are compared with the experimental value. In this way, the partial width Γ_0 was determined as

$$\Gamma_0 = (7.3 \pm 0.6) \times 10^{-3} \text{ eV}.$$

This value is considerably higher than the result $\Gamma_0 = 5.92 \times 10^{-3}$ eV of another self-absorption experiment.² However, when the experimental points shown in Fig. 3 of Ref. 2 were reanalyzed using an appropriate modification of Eq. (2), a value $\Gamma_0 = 7.1 \times 10^{-3}$ eV, which is in much better agreement with our result, was obtained. Taking into account the curvature in the emission line at zero speed would further increase the value of Γ_0 deduced from the experiment of Ref. 2, and might lead to a value of Γ_0 which is even slightly larger than our result.

From the decomposition of the pulse-height dis-

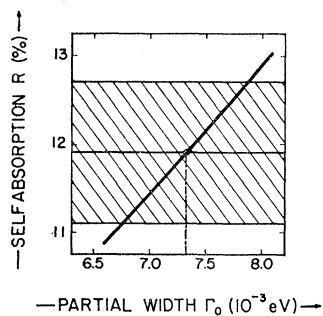


FIG. 4. Sm^{152} : Comparison of the calculated self-absorption (oblique line) with the range of experimental values (shaded area) measured with a Sm_2O_3 absorber of 2.34 g/cm^2 .

tribution of the incident gamma-ray beam and of the resonance-scattered radiation into the contributions of the 0.96- and 0.84-MeV lines, and taking into account the effects of the angular distributions and of the absorption in the scatterer, a value $\Gamma_{0.96}/\Gamma_{0.84} = 0.77 \pm 0.04$ was obtained. This is to be compared with ratios of 0.714² and 0.80¹¹ used elsewhere. The ratio $\Gamma_{0.96}/\Gamma_{0.84} = 0.77$ corresponds to $\Gamma_0/\Gamma = 0.435$ and, with our value for Γ_0 , leads to a total width $\Gamma = (1.7 \pm 0.2) \times 10^{-2} \text{ eV}$ for the 0.96-MeV level in Sm^{152} . The mean lifetime of this level is, therefore,

$$\tau_{\text{level}} = (3.9 \pm 0.4) \times 10^{-14} \text{ sec.}$$

B. Slowing Down in $(\text{Eu}^{152})_2\text{O}_3$

The resonance scattering from Sm^{152} , measured for different rotor speeds, i.e., as a function of the energy difference ΔE between the centers of the emission and absorption lines, is compared in Fig. 5 with the scattering expected for a collision-free source. The resonance effects are plotted at the abscissae corresponding to the respective tangential source velocities, although the measurements as well as the calculations were averaged over emission angles differing by as much as 30° from the tangential direction. In calculating the collision-free curve, the energy available for the electron-capture transition was assumed⁶ to be 0.94 MeV, and the ratio of K capture to L capture, seven to one.

Figure 5, showing a large difference between the observed shape and the collision-free shape, demonstrates that, even for a lifetime as short as $3.9 \times 10^{-14} \text{ sec}$, the slowing down effects are sizeable. The extension of the data of Moon and Shute⁶ to smaller values of ΔE , made possible by the higher operational speed of our rotors, clearly proves that the observed resonance effect does not level off as the gap between emission and absorption lines is reduced, but increases monotonically, in sharp contrast to the collision-free curve and to the extrapolation used in Ref. 6.

In evaluating the slowing down information contained in Fig. 5, we shall concentrate on the most energetic recoils, i.e., on those which contribute to the region near the end points of the emission line. We

then use the simple picture^{8,12} that these recoils move with essentially their initial velocities for a time τ_c , and that they are then removed rather abruptly from their original high-momentum interval. Since the thermal velocities are one order of magnitude smaller than those of this select group of recoils, and since collisions between fast recoils are extremely rare, it is very improbable for a low-energy recoil to be promoted to the high-momentum group. This means that the emission line, while being decimated near the end point, will preserve to a considerable extent its original shape in this region. If the nuclear lifetime is designated by τ_n , the intensity near the end points, in units of the collision-free intensity, is given by the fraction of excited states which decay within the collision-free time τ_c , i.e., by

$$F = 1 - \exp(-\tau_c/\tau_n). \quad (3)$$

For $\tau_c \ll \tau_n$, this becomes $F = \tau_c/\tau_n$. This simple picture has obtained considerable support by rather extensive theoretical studies¹³ of the trajectories of copper recoils in a copper lattice, studies that led to a satisfactory description of the resonance yield from solid copper sources.¹⁴

Of course, if one moves farther away from the end points towards the center of the emission line, the depletion will be partially offset by filling-in from regions closer to the endpoints, and one will reach a point ($\Delta E \approx 3 \text{ eV}$ in Fig. 5) where removal and filling-in are in balance.

Above $\Delta E = 5.5 \text{ eV}$, the experimental curve and the

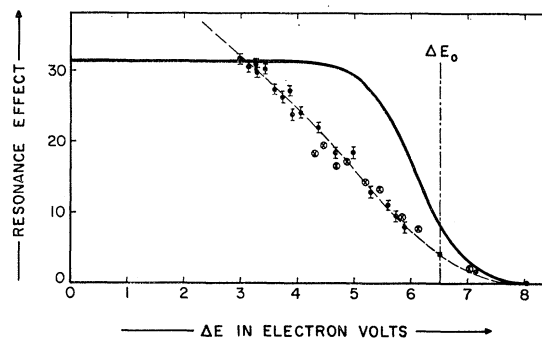


FIG. 5. Sm^{152} : Resonance scattering from the 0.96-MeV level for different values ΔE of the separation of the absorption line from the center of the emission line. With source and absorber at rest, the absorption line center (ΔE_0) is 6.52 eV above the center of the emission line. Our experimental points (●) for different rotor speeds, i.e., for different values of ΔE , are compared with the results of Ref. 6 (⊗) and with the expected behavior (solid curve) for a collision-free Eu^{152} source. The points to the right of ΔE_0 were obtained with the source moving away from the scatterer, those on the left of ΔE_0 with the source moving towards the scatterer. One electron volt corresponds to 813 rps.

¹² K. Ilakovac, Proc. Phys. Soc. (London) **A67**, 601 (1954).

¹³ J. B. Gibson, A. N. Goland, M. Milgram, and G. H. Vineyard, Phys. Rev. **120**, 1229 (1960).

¹⁴ J. B. Cumming, A. Schwarzschild, A. N. Sunyar, and N. T. Porile, Phys. Rev. **120**, 2128 (1960).

¹¹ Nuclear Data Sheets, compiled by K. Way et al. (Printing and Publishing Office, National Academy of Sciences—National Research Council, Washington 25, D. C.) NRC59-4-86.

collision-free curve in Fig. 5 have approximately the same shape, the experimental points being lower by a factor of 2.3. This means that the factor F in Eq. (3) has the value $F=1/2.3=0.435$. With $\tau_n=3.9\times 10^{-14}$ sec, Eq. (3) then yields $\tau_c=2.2\times 10^{-14}$ sec. Since the velocity of the fast recoils is $v=2\times 10^5$ cm/sec, the distance traveled by the recoils during the collision-free time is 4.4×10^{-9} cm. This value is in accord with reported collision-free distances of 3.10^{-9} cm for Re^{187} in tungsten⁷ and of 10.10^{-9} cm for Ce^{140} in La_2O_3 .⁸ In the Re^{187} case, a smaller distance is expected because of the tighter lattice and the fact that all collisions take place between atoms of equal mass. The value for Ce^{140} is an upper limit since the experiment was carried out without an ultracentrifuge, and the transition energies are such that the absorption line falls into a region of the emission line where filling-in from higher momentum recoils leads to a larger resonance effect and hence an overestimate of the collision-free distance. For the following we shall use the value 4.4×10^{-9} cm for the collision-free distance in rare-earth oxides.

C. Scattering from Sm^{148}

The results of the scattering experiments with Sm^{148} are summarized in Fig. 6 where the resonance effect is plotted versus the rotor speed. Near the end point of the emission line, which, in this case, almost coincides with the zero-speed point, the shape of the collision-free resonance effect versus rotor-speed curve was fitted to the experimental data and is shown in Fig. 6 as the heavily drawn curve. Beyond approximately 1600 rps, the measured points deviate from this curve, thus showing evidence for filling-in through slowing down. For the fit indicated in Fig. 6, a value $F\Gamma_0^2/\Gamma=1.8\times 10^{-4}$ eV was used, the uncertainty in this value being $\pm 40\%$. Using the collision-free distance of 4.4×10^{-9} cm measured for Sm^{152} , and a recoil velocity of 2.9×10^5 cm/sec, the collision-free time τ_c for the Sm^{148} case becomes 1.5×10^{-14} sec. Since this is considerably shorter than the

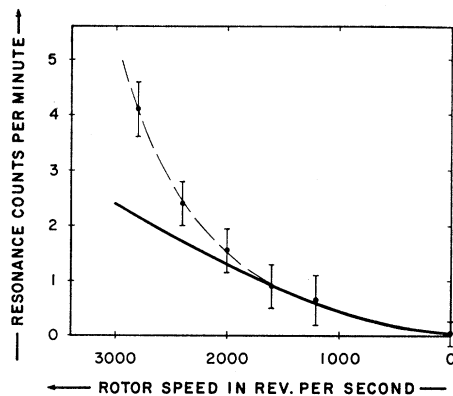


FIG. 6. Sm^{148} : Resonance scattering from the 1.46-MeV level for different rotor speeds. The heavily drawn curve represents the best fit, using the shape of the collision-free curve (Fig. 1), to the experimental points below 2000 rps.

lifetime of the level—the small scattering effect and the strong filling-in attest to that— F may be approximated by the ratio τ_c/τ_n . With this, the result of the scattering experiment may be written as

$$F\Gamma_0^2/\Gamma = (\tau_c/\tau_n)(\Gamma_0^2/\Gamma) = \tau_c\Gamma_0^2/\hbar = (1.8\pm 0.7)\times 10^{-4} \text{ eV},$$

giving for the partial width Γ_0 of the ground-state transition the value

$$\Gamma_0 = (2.8\pm 0.6)\times 10^{-3} \text{ eV}.$$

The error quoted above does not include the uncertainty in the collision-free time τ_c . Since Γ_0 is inversely proportional to the square root of τ_c , the error in Γ_0 will be changed only from 0.6×10^{-3} to 0.8×10^{-3} eV, if one assigns an uncertainty of $\pm 30\%$ to τ_c .

Using the larger error for Γ_0 and the ratio $\Gamma_0/\Gamma=0.61$,¹⁵ one obtains for the total width of the 1.46-MeV level in Sm^{148} the value

$$\Gamma = (4.6\pm 1.3)\times 10^{-3} \text{ eV},$$

corresponding to a mean lifetime

$$\tau_{\text{level}} = (1.4_{-0.3}^{+0.6})\times 10^{-13} \text{ sec}.$$

D. Angular Distribution of the Sm^{148} Resonance Radiation

In an effort to ascertain that the observed resonance scattering from Sm^{148} originated from the 1.46-MeV spin-1 level, the data taken at a scattering angle of 105° were supplemented by data taken at 130° . The results are summarized in Table I.

TABLE I. Comparison of the observed ratio $W(130^\circ)/W(105^\circ)$ of the resonance counting rates at scattering angles 130° and 105° with the ratios calculated for different spin assignments to the level in Sm^{148} which is responsible for the resonance scattering.

Assumed spin of excited state	Theoretical ratio $W(130^\circ)/W(105^\circ)$	Experimental ratio $W(130^\circ)/W(105^\circ)$
1	1.32	1.52 ± 0.37
2	0.54	

The experimental ratio is only compatible with a spin value of 1 for the level predominantly excited in the resonance fluorescence experiment.

IV. RESULTS AND DISCUSSION

In Table II the transition probabilities of the four gamma-ray transitions, originating from the two levels studied in this paper, are listed and are compared with the single-particle estimates.¹⁶

¹⁵ C. V. K. Baba, G. T. Ewan, and J. F. Suarez, Nucl. Phys. 43, 264 (1963).

¹⁶ J. M. Blatt and V. F. Weisskopf, *Theoretical Nuclear Physics* (John Wiley & Sons, Inc., New York, 1952), Chap. 12.

TABLE II. Summary of the transition probabilities determined in this work, and comparison with the predictions of the single-particle model (Ref. 16).

Nucleus	E_γ (MeV)	Transition	Transition probability (sec ⁻¹)	$B(E1)_d$ ($10^{-29}e^2 \text{ cm}^2$)	$\frac{B(E1)_d}{B(E1)_{sp}}$
Sm ¹⁴⁸	1.46	1 ⁻ → 0 ⁺	$(4.3 \pm 1.2) \times 10^{12}$	0.9	5×10^{-4}
	0.91	1 ⁻ → 2 ⁺	$(2.7 \pm 0.8) \times 10^{12}$	2.3	12×10^{-4}
Sm ¹⁵²	0.96	1 ⁻ → 0 ⁺	$(11 \pm 1) \times 10^{12}$	7.9	4×10^{-3}
	0.84	1 ⁻ → 2 ⁺	$(14 \pm 2) \times 10^{12}$	15.4	8×10^{-3}

The upper limit established recently¹⁷ for the $B(E1)$ of the 1.46-MeV level in Sm¹⁴⁸ by a Coulomb excitation experiment with 43.5-MeV oxygen ions, $B(E1)_d \leq 3 \times 10^{-29}e^2 \text{ cm}^2$, is consistent with our value for the reduced transition probability. As far as the lifetime of the 0.96-MeV state of Sm¹⁵² is concerned, our value falls into the range established by previous experiments.^{2,9,18}

It is evident from Table II that the $B(E1)$ values change rather abruptly as one proceeds from the spherical nucleus Sm¹⁴⁸ to the deformed Sm¹⁵² nucleus. Further measurements of transition probabilities of 1⁻ states in the region of the deformed rare-earth nuclei as well as below neutron number 90 will be

¹⁷ Y. Yoshizawa, B. Elbek, B. Herskind, R. J. Keddy, and M. C. Oleson, *Bull. Am. Phys. Soc.* **9**, 497 (1964).

¹⁸ L. Grodzins, *Phys. Rev.* **109**, 1014 (1958).

necessary in order to establish whether this change in the $B(E1)$'s is accidental or whether it indicates a definite trend.

It might be worth pointing out that the ratio of the $B(E1)$'s for the corresponding transitions in Sm¹⁴⁸ and Sm¹⁵² is approximately the same as the ratio of the $B(E2)$'s for the first 2⁺ states. In addition, the excitation energies of the 1⁻ and the 2⁺ states change by approximately the same amounts as the neutron number changes,¹⁹ while the excitation energies of the 3⁻ states remain practically constant. Since the energies of the 2⁺ states are much lower to start with, the fractional changes upon crossing neutron number 90 are much larger for the 2⁺ states than for the 1⁻ states.¹ The relationships mentioned above may be of interest in view of the suggestion that some of the 1⁻ levels in even-even nuclei arise from the coupling of a quadrupole and an octupole collective excitation.²⁰

ACKNOWLEDGMENT

The author would like to thank Dr. S. Fallieros for several helpful discussions.

¹⁹ R. A. Kenefick and R. K. Sheline, *Phys. Rev.* **135**, B939 (1964).

²⁰ K. Alder, A. Bohr, T. Huus, B. Mottelson, and A. Winther, *Rev. Mod. Phys.* **28**, 432 (1956); see also: A. Bohr and B. Mottelson, *Nucl. Phys.* **4**, 529 (1957).

Alpha Clusters in a Harmonic-Oscillator Potential

F. C. CHANG

Physics Department, St. John's University, Jamaica, New York

(Received 28 September 1964; revised manuscript received 17 November 1964)

The probabilities of occurrence of alpha clusters are calculated for the case of four nucleons in a harmonic-oscillator potential, based on the simplifying approximation that the oscillator constants for alpha clusters and nucleons are equal. Some general observations as to how alpha-decay hindrance is affected by the overlap of wave function of a cluster and that of the constituent nucleons are made. The decay of Po²¹¹ is discussed in part.

I. INTRODUCTION

IN the shell model the hindrance of alpha decay can be attributed to a number of factors. In this paper we shall study one of these, namely, the overlap of wave function of an alpha cluster and that of the constituent nucleons. Other factors include centrifugal barrier, configuration mixing, coefficient of fractional parentage, etc.

Consider the motion of two protons and two neutrons in a harmonic-oscillator potential. Their wave function can be written as a linear combination of wave functions, corresponding to various groupings of the nucleons, such as an alpha cluster; it has the form

$$\Psi = \sum_i a_i \Psi_i, \quad (1)$$

where Ψ_i are wave functions for the various groupings, and $|a_i|^2$ is the probability of occurrence of grouping i . We shall calculate the coefficients a_i for the alpha groupings.

II. CALCULATIONS

The Hamiltonian for four nucleons in a harmonic-oscillator potential is

$$H = \frac{1}{2m} \sum_{i=1}^4 p_i^2 + \frac{1}{2} m \omega^2 \sum_{i=1}^4 r_i^2, \quad (2)$$

where \mathbf{r}_i and \mathbf{p}_i are the coordinates and momenta of the nucleons and m the nucleon mass.

The quantum numbers for orbital angular momentum and total angular momentum of nucleon i shall be